

Original paper

Provenance of Jurassic–Cretaceous siliciclastic rocks from the northern Siberian Craton: an integrated heavy mineral study

Oleg S. VERESHCHAGIN^{1*}, Andrey K. KHUDOLEY¹, Victoria B. ERSHOVA¹,
Andrey V. PROKOPIEV², Gennady V. SCHNEIDER³

¹ St. Petersburg State University, Institute of Earth Sciences, Universitetskaya nab. 7/9, 199034, St. Petersburg, Russia;
o.vereshchagin@spbu.ru

² Diamond and Precious Metal Geology Institute, Siberian Branch, Russian Academy of Sciences, Lenin Prospect 39, 677980, Yakutsk, Russia

³ All Russian Geological Research Institute (VSEGEI), Sredniy Prospect 74, St. Petersburg, 199106, Russia

* Corresponding author



The U–Pb ages of detrital zircons and the chemical compositions of detrital garnets and tourmalines from Jurassic–Cretaceous sedimentary rocks of the northern part of the Priverkhoyansk Foreland Basin, the central part of the Yenisey–Khatanga Depression, and the northern part of the Taimyr–Severnaya Zemlya Fold and Thrust Belt were used for a provenance study. Detrital zircons display two age populations, dominated by Late Paleozoic and Paleoproterozoic–Archean zircons, respectively. The first population was recognized in all samples, whereas the second is restricted to Cretaceous samples, suggesting that erosion of the Siberian Craton basement was the main source of clastic sediments only during the Cretaceous. The chemical compositions of the garnets also indicate several sources of detrital material, which changed with time. There are significant differences in the composition of Jurassic (grossular–almandine) and Cretaceous (mainly pyrope) garnets. The pyrope association is characteristic of the high-grade metamorphic rocks of the Siberian Craton, which correlates well with our zircon data. The chemical composition of tourmaline grains varies widely and does not show significant differences between samples of different ages, therefore could not be used to discriminate between different provenance areas in this study.

Keywords: Siberian Craton, provenance, heavy minerals, garnet, tourmaline, zircon

Received: 1 November 2017; **accepted:** 13 June 2017; **handling editor:** M. Novák

The online version of this article (doi: 10.3190/jgeosci.264) contains supplementary electronic material.

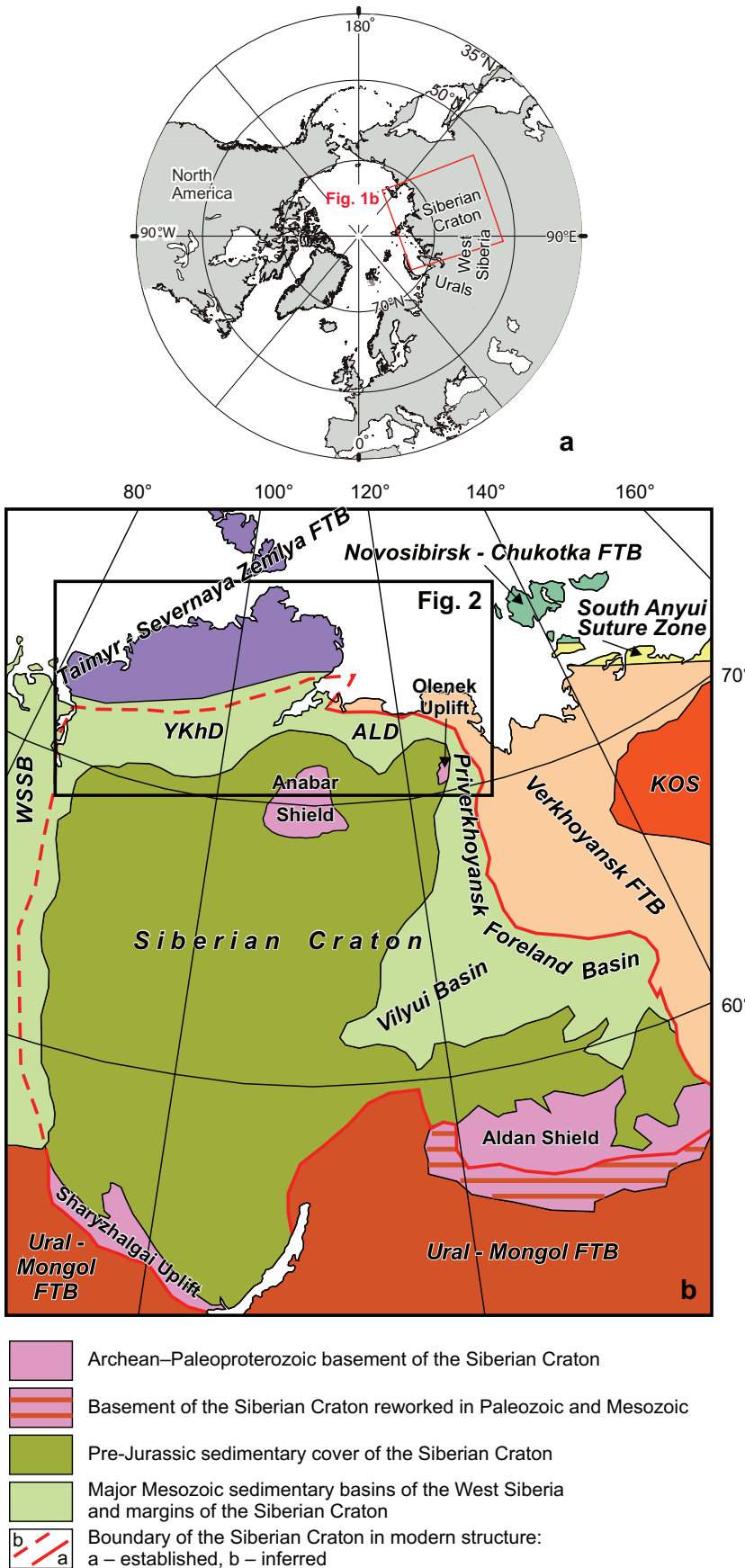
1. Introduction

Clastic sediments contain a record of the composition and evolution of their source area and represent key tie points for validating paleogeographic and paleotectonic reconstructions. U–Pb dating of detrital zircons has emerged as the most popular tool in recent provenance studies and the associated techniques, opportunities and applications were summarized in a set of recent papers (Cox 2003; Fedo et al. 2003; Anderson 2005; Cawood et al. 2012; Gehrels 2012, 2014). The method focuses on identification of the age of magmatic and/or metamorphic rocks in the source area. However, as zircons are highly resistant to physical abrasion and chemical weathering, it is likely that they have been recycled several times by sedimentary reworking, adding extra complexity to an interpretation of their provenance. Some rock types, such as mafic and ultramafic magmatic rocks, contain few zircons. Therefore, sediment contributions from such rocks may be missed or misinterpreted by detrital zircon studies. Furthermore, U–Pb dating of detrital zircons cannot directly provide reliable information on the rock type in the provenance area, for which other geochemi-

cal techniques are required. One such technique is heavy minerals analysis, discussed in detail by Morton (1985, 1991) and Mange and Morton (2007).

The most reliable technique for understanding the principal rock types in a source area of sediment is an analysis of the chemical composition of tourmalines and garnets (e.g. Henry and Guidotti 1985; Hallsworth and Chisholm 2008; Kowal-Linka and Stawikowski 2013; Vďačný and Bačík 2015). In most previous studies, detrital tourmaline was represented by grains of dravite and schorl (with rare occurrences of uvite and Mg-foitite), principally derived from metapelites and metapsammites (with a subordinate proportion of grains from Li-poor granitoids). Detrital garnets are more chemically heterogeneous which makes it easier to reconstruct rock types in a provenance area; however, it is still difficult based on standard diagrams (e.g. Kowal-Linka and Stawikowski 2013; Krippner et al. 2014). Nevertheless, with simultaneous use of data from both minerals, the reliability and confidence in resulting paleogeographic and paleotectonic reconstructions are significantly increased.

This paper combines U–Pb detrital zircon dating and heavy mineral analysis to evaluate the provenance of



Jurassic and Cretaceous sandstones in the Mesozoic sedimentary basins framing the northern margin of the Siberian Craton. The only comprehensive heavy mineral study (Kaplan 1976) was carried out more than 40 years ago and is in urgent need of revision with modern approaches. More recent studies (Zhang et al. 2013, 2015; Malyshev et al. 2016) were focused on discrete localized areas and did not attempt to correlate tectonic events between the sedimentary basins along the northern margin of the Siberian Craton.

2. Geological setting

The study area is located along the northern margin of the Siberian Craton and surrounding fold and thrust belts (FTB) (Fig. 1). The Siberian Craton basement consists of Archean terranes that were accreted during the Paleoproterozoic (1.8–1.95 Ga) (Smelov and Timofeev 2007). Major exposures of the Archean and Paleoproterozoic crystalline rocks are found in the Anabar Shield and Olenek Uplift in the northern part of the craton, and the Aldan Shield and Sharyzhalgai Uplift in the southern part. The overlapping sedimentary cover started to form in the Mesoproterozoic. The Meso- and Neoproterozoic sedimentary succession has a patchy distribution within the Siberian Craton, mainly comprising carbonates and clastic unit (Khudoley et al. 2007, 2015 and references therein).

Regional transgression started in the Ediacaran and led to deposition of Ediacaran–Lower Paleozoic, predominantly shallow-marine carbonates and evaporites across a large part of the craton. In the Late Devonian, rifting occurred along the eastern margin of

Fig. 1 Simplified geological map of the Siberian Craton and adjoining fold and thrust belts and sedimentary basins. Possible source areas for clastic material and location of the study area are also shown. FTB – Fold and Thrust Belt, YKhd – Yenisey–Khatanga Depression, ALD – Aldan–Lena Depression, WSSB – West Siberian Sedimentary Basin, KOS – Kolyma–Omolon Superterrane.

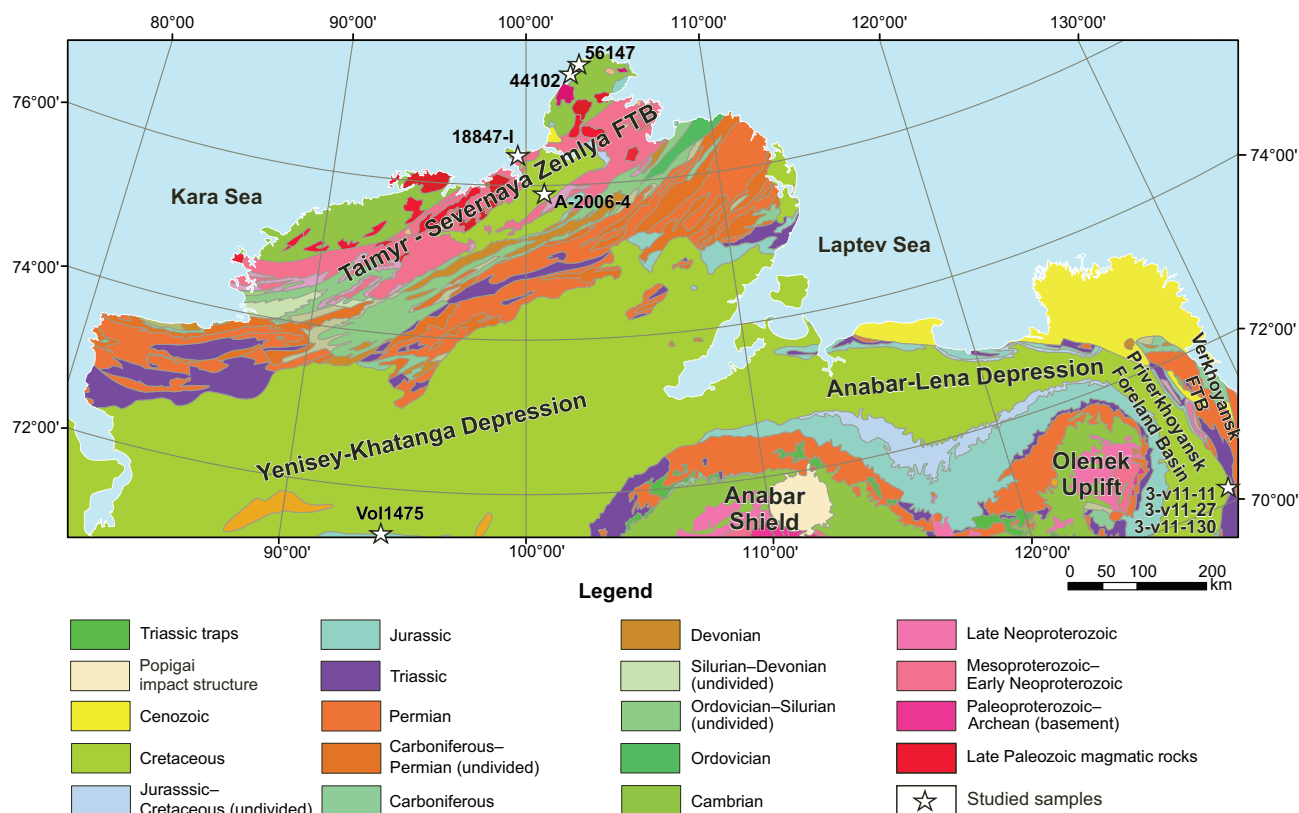


Fig. 2 Geological map showing location of samples within the Mesozoic sedimentary basins at the northern margin of the Siberian Craton. Geology after Pogrebitsky (1998), Malich (1999) and Ershova et al. (2016) (modified). Samples 19-v09-8 and 19-v09-81 and samples 3-v11-11, 3-v11-27 and 3-v11-130 were collected in adjacent sections (see coordinates in Tab. 1).

the craton, which was followed in the latest Early Carboniferous by a shift from carbonate to mainly clastic sedimentation across the craton as a whole. Since that time, a thick clastic succession was deposited along the subsiding northern and eastern passive margins of the craton, while only a thin and patchy Upper Paleozoic–Mesozoic cover was deposited and preserved across the central part (Prokopiev et al. 2001).

The Siberian Craton is framed by thrust and fold belts mainly formed as a result of terrane accretion to the margins of Siberia during the Neoproterozoic–Cretaceous (Fig. 1). They consist mainly of low-grade metamorphic to unmetamorphosed rock units varying in age from Mesoproterozoic to Mesozoic, cut by Neoproterozoic, Late Paleozoic and Mesozoic granite intrusions (Zonenshain et al. 1990; Vernikovskiy 1996; Prokopiev et al. 2001 and references therein).

Mesozoic sediments are widely distributed along the northern margin of the Siberian Craton within the northern Priverkhoyansk Foreland Basin, Anabar–Lena Depression and Yenisey–Khatanga Depression, along with Jurassic and Cretaceous sediments overlapping folded rock units of the Taimyr–Severnaya Zemlya FTB (Fig. 2).

Within the Taimyr–Severnaya Zemlya FTB, the Jurassic and Cretaceous rocks have sub-horizontal bedding

and are represented by poorly lithified shallow marine to fluvial sandstones, with subordinate clays and laterally discontinuous conglomerate and sandstone beds (Fig. 3).

The Yenisey–Khatanga Depression is the deepest sedimentary basin on the northern margin of the Siberian Craton. The Lower Jurassic rocks of the Yenisey–Khatanga Depression unconformably overlie various strata of Triassic age, and consist of shales and siltstones with subordinate fine- to medium-grained sandstones deposited in marine environments. According to seismic data, the total

Tab. 1 Age and location of studied samples

No	Sample No	Coordinates		Age
		latitude	longitude	
1	44102-VII	77°27'16"	102°48'8"	J ₁
2	Vol-1475	71°16'00"	94°40'25"	J ₁
3	44102-VI	77°27'16"	102°48'8"	J ₂
4	56147-XIII	77°32'47"	103°23'21"	J ₂
5	3-v11-11	70°47'48.5"	127°36'52.9"	J ₂
6	19-v09-08	70°57'36.5"	127°30'26.5"	J ₂
7	44102-IV	77°27'16"	102°48'8"	J ₃
8	A-2006-4	75°54'23"	101°05'15"	J ₃
9	3-v11-27	70°47'31.3"	127°36'27.2"	K ₁
10	18847-1	76°24'3"	99°21'35"	K ₁
11	19-v09-81	70°57'02.5"	127°29'06.7"	K ₁
12	3-v11-130	70°47'31"	127°36'27"	K ₁

thickness of Jurassic and Cretaceous rocks reaches up to 10–11 km in the central part of the depression, decreasing towards its margins and northeastward (Afanasenkov et al. 2016). Paleocene sediments are also preserved locally. The origin of the Yenisey–Khatanga Depression was likely related to the latest Permian–Early Triassic rifting event, widespread in adjacent parts of the West Siberian Basin and Siberian Craton (e.g. Botneva and Frolov 1995; Pogrebitskiy and Shanurenko 1998).

The Priverkhoyansk Foreland Basin is located along the eastern margin of the Siberian Craton and extends for ~1100 km, separating the Verkhoysansk FTB to the east from the Siberian Craton to the west (Fig 1). The

Verkhoyansk FTB extends to the east and south as far as to the Pacific coast (Parfenov et al. 1995; Prokopiev et al. 2001; Khudoley and Prokopiev 2007). Folding in the Verkhoysansk FTB resulted from Late Mesozoic collision between the Siberian Craton and the Kolyma–Omolon Superterrane. Changes in sedimentary facies from the Tithonian to Aptian correlate with a switch from distal foredeep to proximal foredeep sedimentation, related to westward migration of depocentres in front of the westward propagating thrust belt (Ershova et al. 2012).

3. Materials and methods

3.1. Sampling

Twelve sandstone samples were selected for U–Pb detrital zircon dating and detrital tourmaline and garnet chemical composition analysis from the Jurassic and Cretaceous succession. Their locations and stratigraphic context are shown in Figs 1, 3 and in Tab. 1. Two areas, located in opposite (northwestern and southeastern) parts of the discussed Mesozoic sedimentary basins, were selected for U–Pb detrital zircon study and tourmaline and garnet chemical composition analysis, in order to identify the likely provenance of Jurassic and Cretaceous strata.

Within the *northern Taimyr* area, six samples were collected for U–Pb detrital zircon and heavy mineral analysis, five Jurassic and one Cretaceous (Fig. 3). The Lower and Middle Jurassic samples are cross-bedded, poorly-sorted, medium- to coarse-grained sublithic to subarkose sands. Upper Jurassic samples represent coarser grained sands and are more mature in composition. The Cretaceous (Albian)

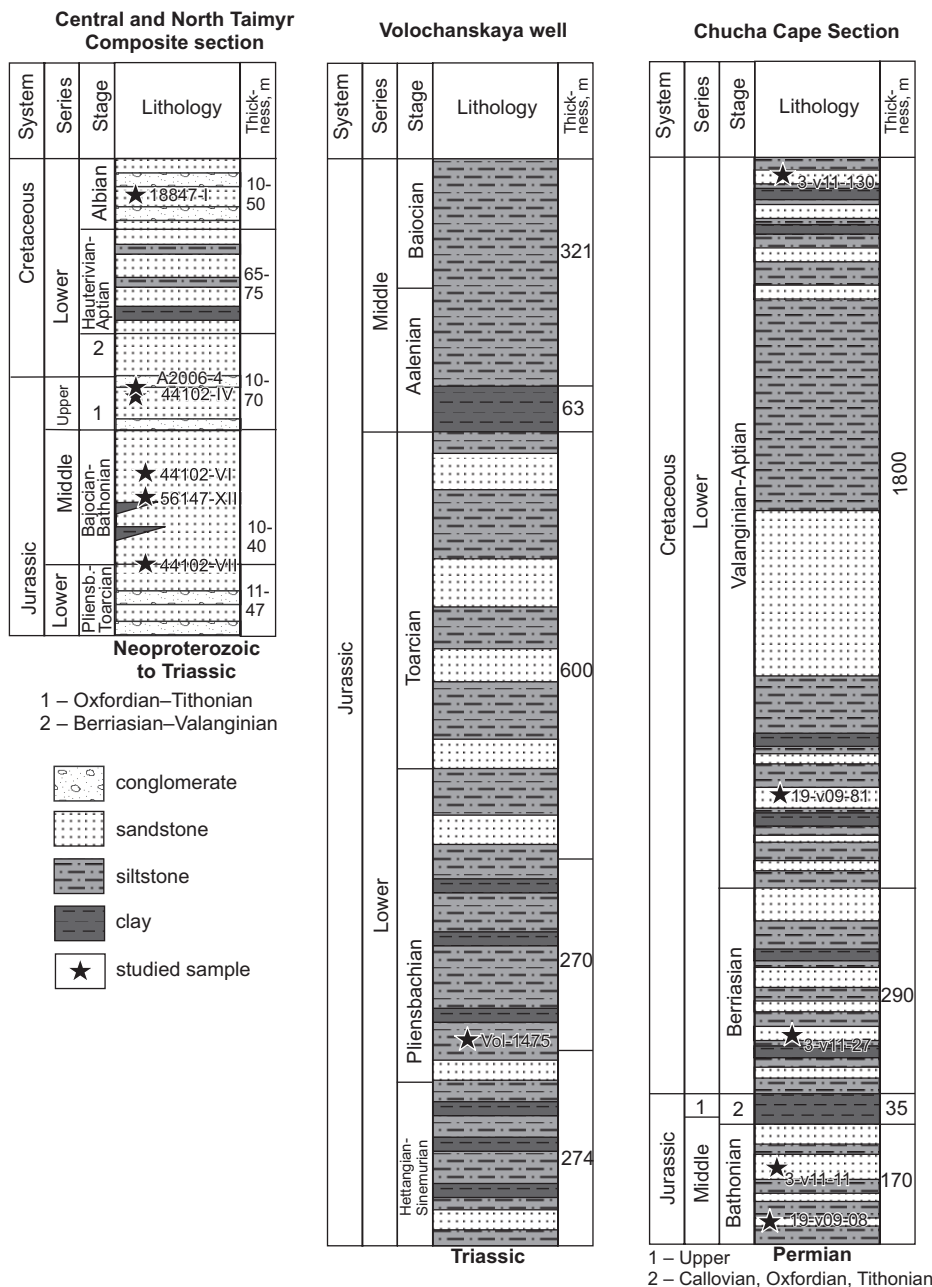


Fig. 3 Stratigraphic chart for studied Jurassic and Cretaceous sections, after Makariev (2013) and data by authors. See location of samples in Fig. 2.

sample is a medium-grained subarkose sandstone. The only studied sample in the *Yenisey–Khatanga Depression* is the Lower Jurassic subarkose sandstone from the Volochanskaya well located in the central part of the depression (Fig. 3). Five samples have been obtained in the northern part of the *Priverkhoyansk Foreland Basin*, two from Middle Jurassic and three from Lower Cretaceous strata (Fig. 3). Middle Jurassic and lowermost Cretaceous samples are medium-grained arkosic to subarkosic sandstones, likely of deltaic origin. Samples from the upper part of the Lower Cretaceous succession (Hauterivian–Aptian) are represented by medium- to coarse-grained cross-bedded fluvial sandstones of arkosic composition.

3.2. U–Pb dating of detrital zircon

Heavy minerals were concentrated at the Institute of Precambrian Geology and Geochronology, Russian Academy of Science (St. Petersburg), using standard techniques including rock crushing to fragments ~0.25 mm size and sorting by density using heavy liquids (bromoform, $\rho = 2.96 \text{ g/cm}^3$, and methylene iodide, $\rho = 3.32 \text{ g/cm}^3$). Prior and after the heavy liquid mineral separation, a magnetic separator was used to remove magnetic minerals.

Zircons were separated from heavy mineral concentrates using Clerici solution ($\rho = 4.15 \text{ g/cm}^3$). The zircon grains from 5 samples (18847-I, 44102-IV, 44102-VII, 19-v09-8 and 19-v09-81) were mounted in epoxy and polished. As the main goal of the U–Pb detrital zircon study was to determine the provenance, zircon grains were selected randomly, irrespective of color, shape, degree of rounding and other features (Fedo et al. 2003; Gehrels 2012). According to Gehrels (2012), a reasonable initial approach for most provenance studies is to conduct U–Pb dating of ~100 detrital zircon grains in each sample.

Laser-ablation ICP-MS (LA-ICP-MS) U–Pb analyses were carried out by Apatite to Zircon Inc. (Viola, ID, USA) with $^{207}\text{Pb}/^{206}\text{Pb}$ ages reported for $> 1.0 \text{ Ga}$ grains and $^{206}\text{Pb}/^{238}\text{U}$ ages for $\leq 1.0 \text{ Ga}$ grains. A detailed description of analytical procedures and data tables with accepted ages are provided in Electronic Supplementary Material 1 and explanation text. Results are illustrated by diagrams with superimposed histograms and probability density curves, which were calculated and plotted using Isoplot version 3.75 (Ludwig 2012). Uncertainties of LA-ICP-MS ages are quoted as 2σ . Age peaks on the age probability density curves were calculated using AgePick Excel macros (Gehrels 2012).

3.3. Mineral chemistry

Garnets and tourmalines were separated from heavy mineral concentrates under a Leica DM 2500P polar-

izing light microscope. The elemental composition of heavy minerals was analyzed by EDS (AZtecEnergy 350, Oxford Instruments) using an automated Hitachi S-3400N electron microscope at the Geomodel Center in RC SPbSU (analyst V.V. Shilovskih), with the following parameters: 20 kV accelerating voltage, 1 nA beam current and 30 s data-collection time (excluding dead time). Precision for major elements is within ~3 % of the actual amount present; that for minor elements is within ~10 %.

Chemical formulae for *tourmalines* were calculated on the basis of 15 ($Y + Z + T$) atoms per formula unit (apfu) considering that: (1) the boron and water contents were not determined and (2) vacancies may occur at the X site. The charge balance was achieved by calculating ideal boron content ($B = 3 \text{ apfu}$) and adjusting single-charged (OH^-) and double-charged (O^{2-}) anions in the V and W sites ($\text{OH} = 31 - \text{F} - \text{O}$), assuming that all of the iron is divalent.

Due to low chromium content, *garnet* analyses were recalculated to five end-members – pyrope (Prp), almandine (Alm), spessartine (Sps), grossular (Grs) and andradite (And) – with the structural formula based on 8 cations. The Fe^{2+} and Fe^{3+} contents were estimated assuming ideal electroneutral garnet stoichiometry.

4. Results

4.1. U–Pb dating of detrital zircons

The studied samples are located in northern Taimyr and the Priverkhoyansk Foreland Basin (Figs 2–3; Tab. 1). Results of the U–Pb dating of detrital zircons are presented in Fig. 4 and data tables in Electronic Supplementary Material 2. In total, 482 grains fit concordance criteria (see Electronic Supplementary Material 1) and have been included to formulate the following interpretation.

4.1.1. Northern Taimyr

Samples 44102-VII, 44102-IV and 18847-I are from northern Taimyr (Fig. 2). Sample 44102-VII was collected from the central part of the Lower–Middle Jurassic succession (Fig. 3). In the age probability plot compilation (Fig. 4a), Late Paleozoic grains predominate, with the most intense peak at 295 Ma comprising 51 out of 100 grains. Two peaks formed by more than three grains are also recognized at 555 and 583 Ma. No Paleoproterozoic or Archean grains were found.

Sample 44102-IV was collected from the lowermost part of the Upper Jurassic–Lower Cretaceous succession and, most likely, is Late Jurassic in age (Fig. 3). One hundred and seven grains were analyzed and the resulting detrital zircon age distribution is very similar to that of sample 44102-VII (Fig. 4b). The most intense peak at 253

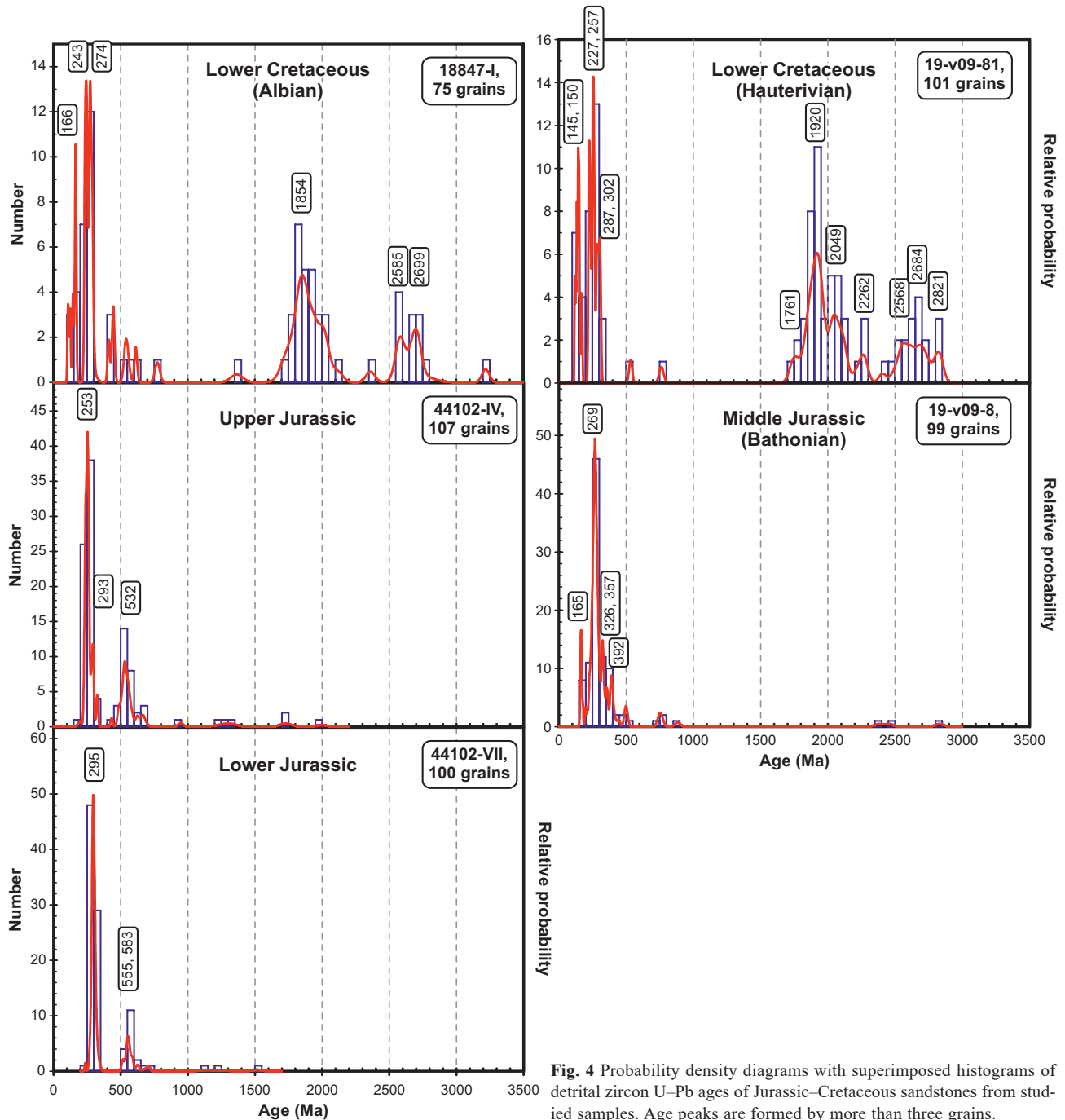


Fig. 4 Probability density diagrams with superimposed histograms of detrital zircon U-Pb ages of Jurassic–Cretaceous sandstones from studied samples. Age peaks are formed by more than three grains.

Ma comprises 34 out of 107 grains. Other peaks formed by more than three grains are recognized at 293 and 532 Ma. Only 6 out of 107 grains are Mesoproterozoic or Paleoproterozoic in age.

Sample 18847-I was collected from the uppermost part of the Lower Cretaceous succession and is Albian in age (Makariev 2013) (Fig. 3). Seventy-five grains were analyzed and the resulting detrital zircon age probability plot is significantly different from those of samples 44102-IV and 44102-VII, characterized by a broad distribution of de-

tritral zircons of Paleoproterozoic and Archean ages forming more than 50 % of the total grain population (Fig. 4c). The most intense peak at 1854 Ma comprises 18 out of 75 grains. Other peaks formed by more than three grains are recognized at 166, 243, 274, 2585 and 2699 Ma.

4.1.2. Priverkhoyansk Foreland Basin

Samples 19-v09-8 and 19-v09-81 are from the northern part of the Priverkhoyansk Foreland Basin (Fig. 2).

Tab. 2 The representative chemical compositions of detrital tourmalines from the samples from Siberian Craton (wt. % and apfu)

Oxide/No	Age, sample No, number of analyzed grains												
	J ₁ , 44102-VII, 26			J ₂ , 44102-VI, 25			J ₃ , 44102-IV, 29			K ₁ , 18847-1, 21			
	1	2	3	4	5	6	7	8	9	10	11	12	
Na ₂ O	2.07	1.75	2.46	2.10	2.28	2.39	1.95	2.21	2.50	2.28	1.93	2.46	
CaO	0.43	0.34	0.54	0.56	0.43	0.61	0.41	0.33	0.51	0.94	0.81	0.97	
K ₂ O	0.00	0.01	0.00	0.01	0.03	0.00	0.02	0.05	0.03	0.01	0.01	0.02	
SiO ₂	35.62	36.33	36.19	36.35	36.85	36.25	35.27	36.66	36.22	36.33	36.31	36.19	
Al ₂ O ₃	33.59	31.14	31.53	30.77	29.98	30.64	33.17	31.35	31.19	32.02	32.43	31.35	
MgO	2.05	7.66	7.22	7.31	8.42	7.26	3.52	7.13	6.94	6.73	6.24	8.12	
TiO ₂	1.02	1.07	0.82	1.08	0.98	0.87	0.77	0.85	0.31	0.67	0.47	0.43	
MnO	0.12	0.03	0.01	0.00	0.00	0.00	0.00	0.00	0.00	0.00	0.00	0.00	
FeO	11.42	6.74	7.22	8.18	7.16	7.98	9.85	7.99	7.99	7.64	7.32	6.63	
F	0.00	0.01	0.00	0.00	0.00	0.00	0.00	0.02	0.01	0.00	0.00	0.00	
O=F	-0.00	-0.01	-0.00	-0.00	-0.00	-0.00	-0.00	-0.02	-0.01	-0.00	-0.00	-0.00	
H ₂ O*	3.56	3.62	3.61	3.64	3.65	3.62	3.52	3.65	3.60	3.62	3.63	3.64	
B ₂ O ₃ *	10.32	10.52	10.48	10.56	10.60	10.49	10.24	10.61	10.46	10.52	10.52	10.56	
Total	100.19	99.22	100.09	100.57	100.38	100.10	98.75	100.85	99.76	100.78	99.66	100.36	
Formulae based on 15 cations (Y+Z+T)													
X	Na	0.68	0.56	0.79	0.67	0.73	0.77	0.64	0.79	0.81	0.73	0.62	0.79
	Ca	0.08	0.06	0.10	0.10	0.08	0.11	0.07	0.06	0.09	0.17	0.14	0.17
	K	0.00	0.00	0.00	0.00	0.01	0.00	0.00	0.01	0.01	0.00	0.00	0.00
	□	0.24	0.38	0.11	0.23	0.18	0.12	0.29	0.14	0.09	0.10	0.24	0.04
Y+Z	Al	6.70	6.05	6.12	5.94	5.79	5.98	6.63	6.05	6.11	6.21	6.35	6.07
	Mg	0.52	1.88	1.78	1.79	2.06	1.79	0.89	1.74	1.72	1.65	1.55	1.99
	Ti	0.13	0.13	0.10	0.13	0.12	0.11	0.10	0.10	0.04	0.08	0.06	0.05
	Mn	0.02	0.00	0.00	0.00	0/00	0.00	0.00	0.00	0.00	0.00	0.00	0.00
T	Fe	1.62	0.93	1.00	1.13	0.98	1.11	1.40	1.09	1.11	1.05	1.02	0.91
	Si	6.02	5.99	5.98	5.97	6.04	6.01	5.98	6.01	6.02	5.99	6.03	5.96
V+W	Al	0.00	0.01	0.02	0.03	0.00	0.00	0.02	0.00	0.00	0.01	0.00	0.04
	F	0.00	0.00	0.00	0.00	0.00	0.00	0.00	0.01	0.01	0.00	0.00	0.00
	OH	3.16	4.00	3.72	3.94	3.99	3.80	3.41	3.90	3.78	3.57	3.56	3.76
B	O	0.84	0.00	0.28	0.06	0.01	0.20	0.59	0.10	0.22	0.43	0.44	0.24
	B	3.00	3.00	3.00	3.00	3.00	3.00	3.00	3.00	3.00	3.00	3.00	3.00
Mg/(Mg + Fe)		0.24	0.67	0.64	0.61	0.68	0.62	0.39	0.62	0.61	0.61	0.60	0.69
x _□ / (x _□ + Na + K)		0.25	0.38	0.13	0.13	0.21	0.14	0.28	0.23	0.10	0.10	0.23	0.04

Sample 19-v09-8 was collected from the Middle Jurassic (Bathonian) succession (Fig. 3). Ninety-nine grains were analyzed and the age distribution (Fig. 4d) resembles samples 44102-VII and 44102-IV, with the most intense peak at 269 Ma comprising 29 out of 99 grains. Other peaks formed by more than 3 grains are recognized at 165, 326, 357 and 392 Ma. Only three out of 99 grains are Paleoproterozoic or Archean in age.

Sample 19-v09-81 was collected from the Lower Cretaceous (Hauterivian) succession (Fig. 3). One hundred and one grains were analyzed to produce the probability plot compilation, and the detrital zircon age distribution is different from that in sample 19-v09-8 but similar to the distribution in sample 18847-I (Fig. 4e). Paleoproterozoic and Archean grains comprise 64 out of 101 grains, with the most intense peaks at 1920 and 2049 Ma. Other peaks formed by more than three grains are recognized at 150, 227, 257, 287, 302, 1761, 2262, 2568, 2684 and 2821 Ma.

4.2. Chemical composition of detrital tourmalines

The chemistries of 101 tourmalines and 302 garnets was analyzed. The analyzed tourmalines and garnets have homogenous compositions and do not display conspicuous chemical zoning.

One hundred and one detrital tourmaline grains were extracted from four samples collected from different stratigraphic levels of the Jurassic–Cretaceous succession of northern Taimyr (northern and central zones of the Taimyr–Severnaya Zemlya FTB, Vernikovskiy 1996) (Figs 2–3, Tab. 1). The grains include irregular, sub-angular, or sub-rounded crystal fragments. In all cases the grains are free of inclusions and are brown-greenish in thin section. The BSE images of tourmaline grains display no evidence of chemical zonation.

According to EDS (Tab. 2), all tourmalines belong to the alkali tourmaline primary group (Fig. 5), in which Na

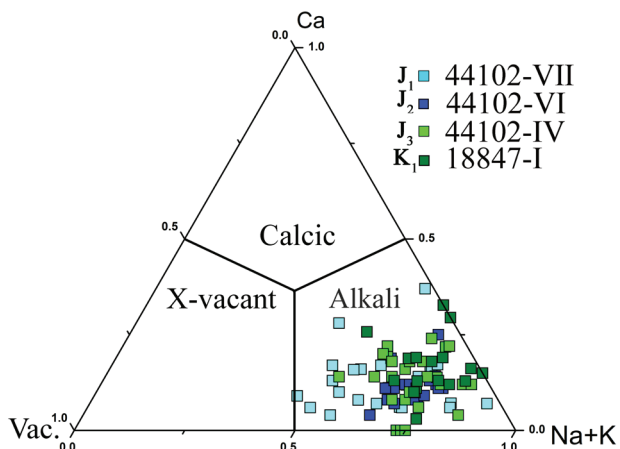


Fig. 5 Chemical composition of detrital tourmalines in the X-site vacancy vs. Ca vs. (Na + K) ternary diagram (Henry et al. 2011; primary groups).

(0.46–0.91 apfu) strongly predominates over K (≤ 0.06 apfu). The content of Ca varies significantly (0.04–0.37 apfu). Regarding the *W*-site occupancy, the studied tourmalines could be divided into two groups. Most (~75 %) are hydroxy-species and belong to alkali-subgroup 1 (dravite and schorl; Fig. 6). Tourmalines represented by oxy-species, belonging to alkali-subgroup 3 (oxy-dravite and oxy-schorl), are less abundant. The latter tourmalines have rather low proportion of X-site vacancies and high Al contents (Fig. 7).

The Mg/(Mg + Fe) ratio varies widely from 0.24 to 0.75 (Fig. 6), which suggests that the tourmaline grains are characterized by various chemical compositions.

Tourmalines from Lower Jurassic (44102-VII), Middle Jurassic (44102-VI), Upper Jurassic (44102-IV) and Lower Cretaceous (18847-1) strata display mutually very similar chemical features and ranges in chemical composition (Tab. 2). There are no significant variations in F, Mn, or Ti contents in the studied samples. They contain more than 6 apfu of Al³⁺ (Tab. 2), which means

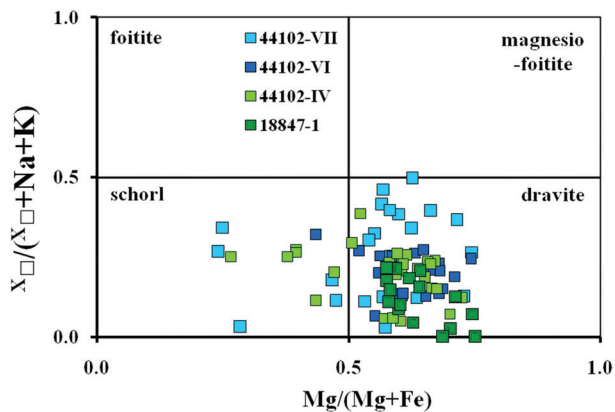


Fig. 6 Chemical composition of detrital tourmalines in the $X_{\square}/(X_{\square} + Na + K)$ vs. $Mg/(Mg + Fe)$ diagram (X_{\square} is X-site vacancy).

that Al occupies both *Y* and *Z* octahedral sites. Correct distribution of magnesium, iron, manganese and titanium ions over two non-equivalent octahedral sites (YO_6 and ZO_6) cannot be established without single-crystal XRD refinement.

Tourmalines from the Lower Jurassic succession (44102-VII; Tab. 2) show the greatest proportion of vacancies in the X-site (up to 0.5 apfu). Tourmalines from the uppermost part of the Lower Cretaceous succession (18847-1; Tab. 2) are the most homogeneous, with the entire population consisting of dravites with high Na content (≥ 0.7 apfu).

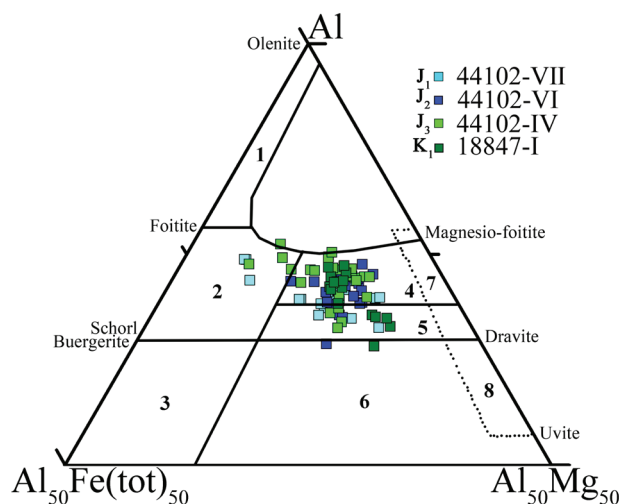


Fig. 7 Chemical composition of detrital tourmalines in the $Fe(tot)_{50}$ –Al– Mg_{50} ternary diagram. Fields 1–8 indicate the compositional ranges of tourmalines from various rock types: 1 – Li-rich granitoid pegmatites and aplites; 2 – Li-poor granitoids and associated pegmatites and aplites; 3 – Fe³⁺-rich quartz–tourmaline rocks (hydrothermally altered granites); 4 – metapelites and metapsammites coexisting with an Al-saturated phase; 5 – metapelites and metapsammites not coexisting with an Al-saturated phase; 6 – Fe³⁺-rich quartz–tourmaline rocks, calc-silicate rocks, and metapelites; 7 – low-Ca metaulttramafic and metasedimentary rocks rich in Cr and V; 8 – metacarbonates and metapyroxenites (after Henry and Guidotti 1985).

4.3. Chemical composition of detrital garnets

Three hundred and two detrital garnet grains were extracted from ten samples (Figs 2–3, Tab. 1). The garnets are predominantly represented by irregular sub-rounded fragments of crystals. None of the grains shows significant dissolution. The grains are free of inclusions and are yellow- or rose-colored in thin section.

The BSE images of garnet grains show no chemical zonation. Variations in the contents of four main end members, almandine [$Alm = Fe^{2+}/(Fe^{2+} + Mg + Ca + Mn)$], pyrope [$Prp = Mg/(Fe^{2+} + Mg + Ca + Mn)$], grossular [$Grs = Ca/(Fe^{2+} + Mg + Ca + Mn)$], and spessartine [$Sps = Mn/(Fe^{2+} + Mg + Ca + Mn)$], observed between

Tab. 3 The representative chemical compositions of detrital garnets from the samples from Siberian Craton (wt. % and apfu)

No/group	Age, sample No, number of analyzed grains									
	J ₁ , 44102-VII, 30		J ₁ , Vol-1475, 31		J ₂ , 44102-VI, 28		J ₂ , 56147-XIII, 29		J ₂ , 3-v11-11, 22	
	1/1	2/2	3/1	4/2	5/1	6/2	7/1	8/2	9/1	10/2
SiO ₂	37.51	36.80	36.83	37.37	38.12	37.41	37.98	37.29	38.37	38.22
TiO ₂	0.00	0.00	0.00	0.00	0.00	0.00	0.00	0.00	0.04	0.00
Al ₂ O ₃	20.94	21.11	20.23	21.22	21.09	21.60	21.61	21.02	21.33	21.05
Cr ₂ O ₃	0.00	0.19	0.00	0.00	0.00	0.00	0.00	0.00	0.06	0.00
FeO	33.15	27.97	34.15	27.16	32.52	24.15	34.12	28.60	33.13	23.83
Fe ₂ O ₃	0.37	0.70	2.51	0.00	0.97	0.10	0.32	0.98	0.00	0.74
MnO	3.59	6.29	1.42	8.79	1.83	6.58	1.58	5.74	1.35	2.27
MgO	3.59	2.24	3.81	1.66	5.36	1.42	4.70	3.56	5.68	2.77
CaO	1.32	4.39	1.26	4.34	1.20	8.84	1.01	2.97	0.89	11.37
Total	100.47	99.99	100.21	100.53	101.09	100.10	101.32	100.16	100.86	100.25
Formulae based on 8 cations										
Si	3.00	2.97	2.96	3.00	3.00	2.98	2.99	2.98	3.01	3.00
Ti	0.00	0.00	0.00	0.00	0.00	0.00	0.00	0.00	0.00	0.00
Al	1.97	2.01	1.92	2.01	1.95	2.03	2.00	1.98	1.97	1.95
Cr	0.00	0.01	0.00	0.00	0.00	0.00	0.00	0.00	0.00	0.00
Fe ²⁺	2.22	1.89	2.29	1.82	2.14	1.61	2.25	1.91	2.18	1.57
Fe ³⁺	0.02	0.05	0.17	0.00	0.06	0.01	0.02	0.07	0.00	0.05
Mn	0.24	0.43	0.10	0.60	0.12	0.44	0.11	0.39	0.09	0.15
Mg	0.43	0.27	0.46	0.20	0.63	0.17	0.55	0.42	0.67	0.32
Ca	0.11	0.38	0.11	0.37	0.10	0.76	0.09	0.25	0.08	0.96
Total	8.00	8.00	8.00	8.00	8.00	8.00	8.00	8.00	8.00	8.00
Content of end-members (mol. %)										
Prp	14	9	15	7	21	6	18	14	22	11
Alm	74	63	77	61	71	54	75	64	73	52
Grs	4	13	4	12	3	25	3	8	3	32
Sps	8	14	3	20	4	15	4	13	3	5
And	0	1	1	0	0	1	0	1	0	0

the inner and marginal parts of the grains, are usually below 1 mol. %.

Chemical composition of the studied detrital garnets varies significantly (Alm_{5–85}Prp_{0–64}Grs_{1–43}Sps_{0–44}). Based on molar Prp/Alm, Sps/Alm and Grs/Alm ratios, all studied detrital garnets could be divided into three groups. The first is represented by almandines with low Mn + Ca (Prp/Alm ≤ 0.5, Sps/Alm ≤ 0.5 and Grs/Alm ≤ 0.5), the second by almandines with high Mn + Ca (Prp/Alm ≤ 0.5, Sps/Alm > 0.5 or Grs/Alm > 0.5), and the third by almandines (with very high Mg) to pyropes with low Mn and Ca contents (Prp/Alm > 0.5, Sps/Alm ≤ 0.5 and Grs/Alm ≤ 0.5).

Two hundred and forty-seven detrital garnets from Lower Jurassic (Vol 1475 and 44102-VII), Middle Jurassic (56147-XIII, 3-v11-11 and 44102-VI) and Upper Jurassic–Lower Cretaceous successions (44102-IV, 3-v11-27 and A-2006-4) were analyzed (Tab. 3). These garnets belong to group 1 and, less so, group 2 (Fig. 8a–b). Most of the garnets from group 2 are enriched in both Ca and Mn (Fig. 8a–b).

Fifty-five grains of detrital garnets from the uppermost part of the Lower Cretaceous succession (18847-I and 3-v11-130, Tab. 3) were analyzed, with garnets deter-

mined to belong to each of the three groups (Fig. 8c–d). There is only one grain with high Ca content (group 2). The total numbers of almandines from group 1 and Mg-rich almandines/pyropes from group 3 are almost equal. An interesting feature of garnets from group 3 are very low Ca and Cr contents.

5. Discussion

The current integrated U–Pb dating and geochemical study of the heavy minerals presented in this paper provide additional constraints that can improve previously published Mesozoic paleogeographic reconstructions for the Siberian Craton. U–Pb detrital zircon dating suggests a significant switch in provenance between the Jurassic and Cretaceous sandstones (Fig. 4). Late Paleozoic granite intrusions are not present in the Verkhoyansk FTB located to the east of the Siberian Craton (Khudoley and Prokopiev 2007, and references therein). Therefore, the predominance of detrital zircon grains with peaks at 293–295 Ma suggests an erosion of granite intrusions widely distributed in the Urals and Taimyr-Severnaya Zemlya FTB (Vernikovskiy 1996; Puchkov 2009 and references

Tab. 3 Continued

No/group	Age, sample No, number of analyzed grains											
	J ₃ , 44102-IV, 36		J ₃ , A-2006-4, 32		K ₁ , 3-v11-27, 39		K ₁ , 18847-1, 29			K ₁ , 3-v11-130, 26		
	11/1	12/2	13/1	14/2	15/1	16/2	17/1	18/2	19/3	20/1	21/2	22/3
SiO ₂	37.31	38.19	37.99	37.11	36.89	37.82	37.97	37.62	38.81	36.83	37.69	38.97
TiO ₂	0.00	0.00	0.02	0.00	0.00	0.00	0.00	0.00	0.00	0.00	0.00	0.00
Al ₂ O ₃	21.79	21.54	21.13	20.32	23.68	20.53	21.48	21.26	21.93	21.74	21.36	22.31
Cr ₂ O ₃	0.00	0.00	0.08	0.00	0.00	0.00	0.00	0.01	0.00	0.00	0.00	0.00
FeO	33.68	24.71	33.13	25.37	27.91	23.74	33.83	27.05	26.52	35.64	28.36	21.34
Fe ₂ O ₃	0.27	0.27	0.00	0.00	0.00	0.00	0.00	1.53	1.22	0.57	2.23	2.88
MnO	2.47	5.50	3.25	17.22	2.29	13.92	0.33	3.29	0.46	0.65	0.65	0.78
MgO	3.34	5.14	4.26	0.49	3.66	1.09	5.46	3.97	10.13	3.32	6.47	13.10
CaO	1.91	4.82	1.09	0.54	5.73	4.21	1.26	5.83	1.06	1.40	3.50	0.84
Total	100.77	100.17	100.96	101.05	100.16	101.31	100.33	100.56	100.16	100.14	100.24	100.21
Formulae based on 8 cations												
Si	2.97	3.00	3.01	3.02	2.90	3.03	3.00	2.96	2.97	2.95	2.95	2.92
Ti	0.00	0.00	0.00	0.00	0.00	0.00	0.00	0.00	0.00	0.00	0.00	0.00
Al	2.04	1.99	1.97	1.95	2.20	1.94	2.00	1.97	1.98	2.06	1.97	1.97
Cr	0.00	0.00	0.01	0.00	0.00	0.00	0.00	0.00	0.00	0.00	0.00	0.00
Fe ²⁺	2.24	1.63	2.20	1.73	1.84	1.59	2.23	1.78	1.70	2.39	1.85	1.34
Fe ³⁺	0.02	0.00	0.00	0.00	0.00	0.00	0.00	0.10	0.08	0.04	0.15	0.18
Mn	0.17	0.37	0.22	1.19	0.15	0.95	0.02	0.22	0.03	0.04	0.04	0.05
Mg	0.40	0.60	0.50	0.06	0.43	0.13	0.64	0.47	1.16	0.40	0.75	1.47
Ca	0.16	0.41	0.09	0.05	0.48	0.36	0.11	0.49	0.09	0.12	0.29	0.07
Total	8.00	8.00	8.00	8.00	8.00	8.00	8.00	8.00	8.00	8.00	8.00	8.00
Content of end-members (mol. %)												
Prp	13	20	17	2	14	4	21	17	39	13	25	49
Alm	75	54	73	58	62	52	74	59	56	80	62	45
Grs	5	14	3	2	17	12	4	16	3	4	10	2
Sps	6	12	7	39	6	32	1	7	1	1	1	2
And	1	0	0	0	0	0	0	1	1	2	2	2

therein; Makariev 2013). Granite intrusions (*c.* 250 Ma), documented in the Urals, Taimyr–Severnaya Zemlya FTB and in the outer part of the Norilsk traps field, are the suggested source for Late Permian–Early Triassic detrital zircon grains in the Jurassic sandstones of northern Siberia (Vernikovskiy et al. 2003; Puchkov 2009; Ivanov et al. 2013). However, direct transport of clastic sediments from the Urals to the northern margin of the Siberian Craton seems unlikely based on the abundance of evidence for predominantly marine environments in the northern part of the West Siberian Sedimentary Basin throughout the Jurassic (Vyssotski et al. 2006 and references therein).

However, less abundant *c.* 530–590 Ma detrital zircons are widely distributed in low-grade metasediments from the northern part of the Taimyr–Severnaya Zemlya FTB (Lorentz et al. 2008; Pease and Scott 2009; Ershova et al. 2015, 2017). We therefore propose that the detritus was sourced from the erosion of a major Late Paleozoic mountain belt located in the Taimyr–Severnaya Zemlya FTB area, probably linked in some way with the Urals. A similar detrital zircon age distribution was documented in Permian rocks (Ershova et al. 2016), but a significant contribution of detrital zircons recycled from older sedimentary deposits is unlikely due to the immature

composition of the studied Jurassic clastic sediments. Only a few Paleoproterozoic and Archean detrital zircon grains were documented in Jurassic sandstones, suggesting very little contribution from erosion of the Siberian Craton basement. Samples from the lowermost part of the Cretaceous succession also show a very similar detrital zircon age distribution (Zhang et al. 2013).

By contrast, two sandstone samples from the upper Lower Cretaceous (Hauterivian and Albian) succession contain predominantly Paleoproterozoic and Archean detrital zircon grains (Fig. 4), suggesting a principal switch to the erosion of Siberian Craton basement. A predominant transport direction of clastic sediments from the Siberian Craton to the Yenisey–Khatanga Depression is also supported by seismic studies (Afanasenkov et al. 2016). Late Paleozoic detrital zircon grains still occur, but are subordinate in comparison with those of Paleoproterozoic and Archean age. We cannot discriminate between erosional products of the Anabar and Aldan shields in our study, but the huge volume of Cretaceous rocks filling the sedimentary basins along the northern margin of the Siberian Craton suggests significant erosion of both shield areas. A similar provenance evolution for the Mesozoic clastic sediments along the eastern margin of

the Siberian Craton was recognized by previous Sm–Nd isotopic studies (Malyshev et al. 2016).

Variations in the chemical composition of garnets from Jurassic and Cretaceous successions are in a good agreement with results of U–Pb dating of detrital zircons. There are six different commonly used garnet discrimination diagrams (Wright 1938; Teraoka et al. 1997, 1998; Grütter et al. 2004; Mange and Morton 2007; Aubrecht et al. 2009; Suggate and Hall 2014). Unfortunately, it was shown by

Krippner et al. (2014) that discrimination by these diagrams only works for a small group of garnets and the assignment to a certain type of host rock remains ambiguous. However, based on published data on chemical differences between garnets of different magmatic and metamorphic rocks and consequently various geodynamic settings (e.g. Deer et al. 1997; Dill et al. 2008; Méres 2008; Aubrecht et al. 2009), we infer that the allocated garnet groups in our study (groups 1–3) represent different provenances.

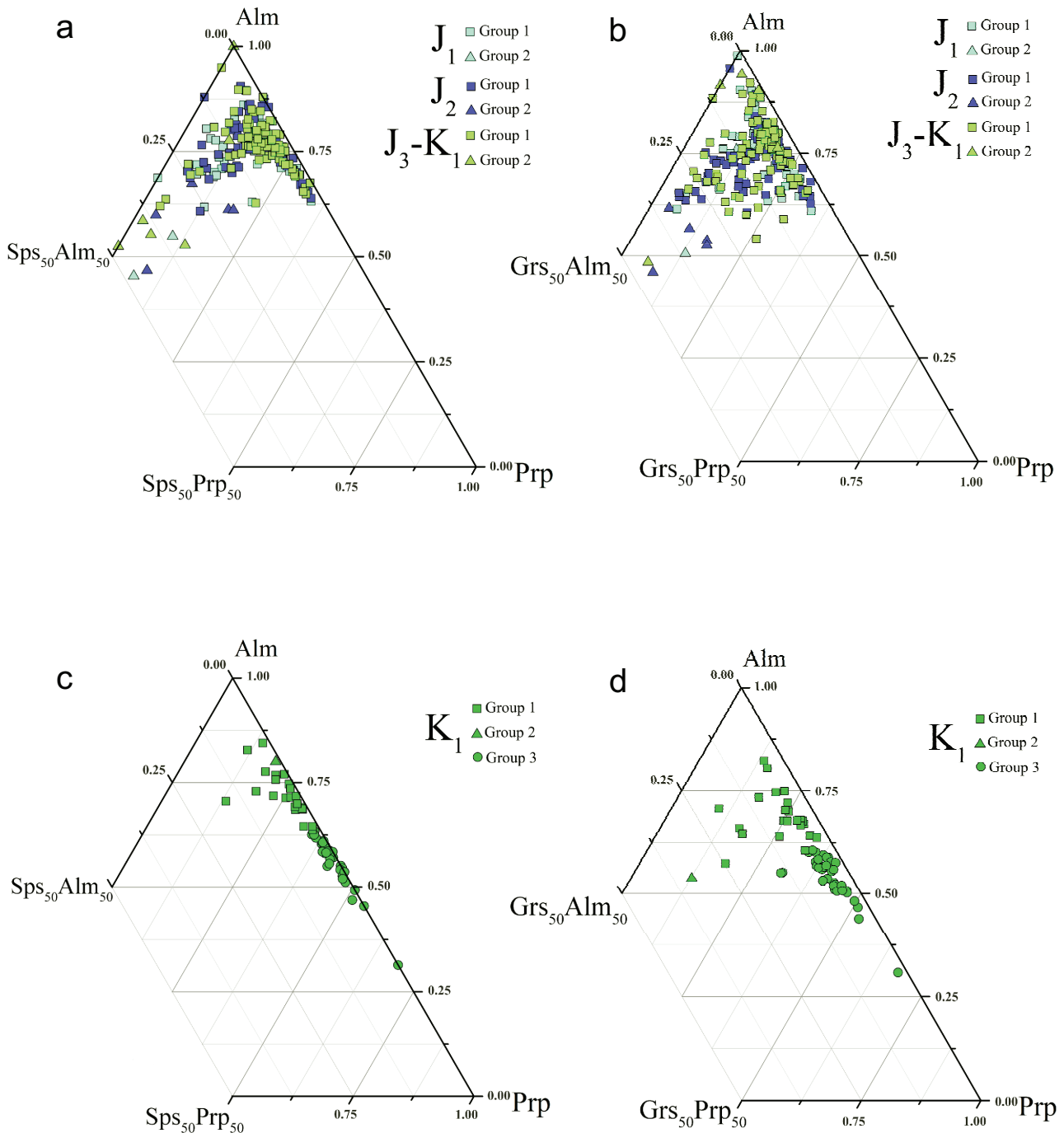


Fig. 8 Chemical composition of detrital garnets in $\text{Sps}_{50}\text{-Alm}_{50}\text{-Prp}$ (a–b) and $\text{Grs}_{50}\text{-Alm}_{50}\text{-Prp}$ (a–b) ternary diagrams.

Garnets from groups 1 and 2 dominate the Jurassic succession. Group 1 consists of almandines with relatively low Mg and Ca contents, suggesting medium- to high-pressure felsic metaigneous rocks as the most probable provenance. Within the northern part of the Taimyr–Severnaya Zemlya FTB, high-pressure felsic rocks have not been documented. However, many granite intrusions with Carboniferous (c. 345–303 Ma) U–Pb zircon ages show significantly younger, Early Permian Ar–Ar biotite and muscovite ages (c. 280–270 Ma). These were interpreted in terms of metamorphic resetting of the Ar–Ar isotopic system (Makariev 2013; Kurapov et al. 2018). Garnets from group 2, with relatively low Mg but high contents of Ca and Mn, could be sourced from mica schists or hornfelses/metasomatic rocks. In summary, garnets from the Jurassic succession were likely derived from metagranites and clastic rocks metamorphosed during Early Permian tectonic event and then widely distributed in the Taimyr–Severnaya Zemlya and Uralian fold and thrust belts, corresponding well with results of our U–Pb detrital zircon study (Vernikovskiy 1996; Puchkov 2009; Makariev 2013).

Garnets from group 3 are found only in the Cretaceous succession and are characterized by a very high Mg content. As proposed by Méres (2008) and Aubrecht et al. (2009), garnets with a pyrope content over 30 mol. % are typical of the eclogite- and high-pressure granulite-facies rocks. According to Grütter et al. (2004), high-Mg and low-Cr garnets can also be derived from uncommon or “polymict” mantle lithologies.

Such high-grade metamorphic rocks are widespread in the basement of the Siberian Craton (Malich 1999; Smelov and Timofeev 2007) and we propose that they were the main source for garnets of group 3. A predominant provenance of Cretaceous sediments from the Siberian Craton basement corresponds well with our detrital U–Pb zircon data (Fig. 4). Also, the large number of pyrope–almandine garnets may indicate the past existence of large high-pressure unit(s), entirely removed during intense Cretaceous erosion across the Anabar and Aldan shields.

In the most commonly used tourmaline provenance diagram (the Fe(tot)–Al–Mg ternary plot by Henry and Guidotti 1985 and van Hinsberg et al. 2011; Fig. 7), compositions of grains from both Jurassic and Cretaceous successions fall predominantly in three fields representing metapelites and metapsammities coexisting (field 4) or not (field 5) with an Al-saturated phase, and Li-poor granitoids with associated pegmatites and aplites (field 2). Two grains (one from the Middle Jurassic and the other from the Lower Cretaceous) straddle the boundary of the field 6 that represents Fe³⁺-rich quartz–tourmaline rocks, calc-silicate rocks and metapelites.

The dravite/schorl ratios indicate that the majority of the grains from both Jurassic and Cretaceous successions

were potentially of metamorphic origin (Kowal-Linka and Stawikowski 2013). Their source material was likely a metasedimentary rock with relatively high boron content. We propose that they were weathered from rocks of variable metamorphic grade up to upper-amphibolite facies, such as paragneisses and micaschists. Some contribution from granite erosion was also possible, but our tourmaline chemical compositional data suggest that a granite source was not significant. The marked changes in age distributions of detrital zircons and chemical composition of garnets from Jurassic to Cretaceous successions do not correlate with data on the chemical composition of detrital tourmalines. No tourmalines related to low-Ca meta-ultramafics, Cr or V-rich metasediments (field 7), or metacarbonates and meta-pyroxenites (field 8) were found. In such rocks tourmaline is usually rare, which might be explanation why they are missing. In the studied samples, the chemical composition of tourmalines seems to be less sensitive to variations in host rocks in the source. There are almost no differences among tourmalines in rocks throughout the Jurassic succession. The Cretaceous sample is slightly different, as it does not contain any tourmaline of Mg/(Mg + Fe) < 0.5 and X-site vacancy > 0.3, but these variations are not sufficient to conclusively separate distinct Jurassic and Cretaceous provenances.

Only a few detrital tourmaline grains were separated from heavy mineral concentrate and analyzed in this study, which was likely related to a lower abundance in source rocks compared to zircon and garnet. This makes interpretation of tourmaline chemistry data less useful. Although the use of tourmalines for provenance studies seems to be very promising, more studies including additional data on REE and isotopic composition are necessary to further characterize tourmalines from different rock types.

6. Conclusions

Our study of heavy minerals in Jurassic–Cretaceous rocks from the sedimentary basins along the northern margin of the Siberian Craton allow us to place new constraints on Jurassic–Cretaceous provenance reconstructions of the Siberian Craton and adjacent areas. In addition it enables to test the application of the garnet and tourmaline chemical compositions as provenance indicators. The main results are the following:

- The composition of garnets from Cretaceous rocks is significantly different from that in Jurassic rocks. Abundant magnesium-rich almandines and pyropes are characteristic of the Cretaceous succession only.
- U–Pb dating of detrital zircons correlates well with the chemical composition of garnets. It suggests that clastic sediments were derived from the Taimyr–Se-

vernaya Zemlya FTB and granite intrusions from the outer part of the Norilsk traps field during the Jurassic. By contrast, clastic sedimentation was sourced mainly from erosion of Siberian Craton basement since the Hauterivian (Early Cretaceous).

- Despite the relatively high variation in chemical composition, tourmalines from rocks of different age occupy the same fields in the discrimination diagrams, suggesting mainly paragneisses and micaschists, with some granite, as a source. Insensitivity of the chemical composition of tourmalines to changes recorded from data on zircons and garnets can be associated with low natural abundance of tourmalines related to low-Ca meta-ultramafics, Cr- or V-rich metasediments, metacarbonates and metapyroxenites.
- Variations in U–Pb detrital zircon ages, as well as chemical compositions of detrital tourmaline and garnet, show very similar trends in the Jurassic and Cretaceous successions in northern Taimyr, the Yenisey–Khatanga Depression, and northern Priverkhoyansk Foreland Basin. We suggest that these provinces were located within a single sedimentary basin in the Mesozoic and were subsequently separated into several discrete basins during Cenozoic tectonic events.

Acknowledgements. The fieldwork and analytical studies done in 2005–2012 were supported by projects with A.P. Karpinsky Russian Geological Research Institute (VSEGEI), TGS, Clapton Research Ltd., and Saint-Petersburg State University. Chemical study of the garnet and tourmaline compositions of samples from the northern Taimyr as well as overall provenance restorations were supported by the Russian Science Foundation grant № 17-17-01171. J. Barnett improved English and supplied useful comments. Constructive reviews by J. Biernacka, R. Čopjaková, J. Cempírek, M. Novák and anonymous reviewer significantly improved the manuscript.

Electronic supplementary material. Description of analytical techniques for U–Pb zircon LA-ICP-MS dating and complete results thereof are available online at the Journal web site (<http://dx.doi.org/10.3190/jgeosci.264>).

References

- AFANASENKOV AP, NIKISHIN AM, UNGER AV, BORDUNOV SI, LUGOVAYA OV, CHIKISHEV AA, YAKOVISHINA EV (2016) The tectonics and stages of the geological history of the Yenisei–Khatanga Basin and the conjugate Taimyr Orogen. *Geotectonics* 50: 161–178
- ANDERSON T (2005) Detrital zircons as tracers of sedimentary provenance: limiting conditions from statistics and numerical simulation. *Chem Geol* 216: 249–270
- AUBRECHT R, MÉRES Š, MIKUŠ T (2009) Provenance of the detrital garnets and spinels from the Albian sediments of the Czorsztyn Unit (Pieniny Klippen Belt, Western Carpathians, Slovakia). *Geol Carpath* 60: 463–483
- BOTNEVA TA, FROLOV SV (1995) Environments of hydrocarbon accumulation in the sedimentary cover of the Enisey–Lena depressions system. *Geol Neft i Gasa* 5: 36–41 (in Russian)
- CAWOOD PA, HAWKESWORTH CJ, DHUIME B (2012) Detrital zircon record and tectonic setting. *Geology* 40: 875–878
- COX RA (2003) Morphological, chemical, and geochronological techniques for characterizing detrital zircon. In: LENTZ DR (ed) *Geochemistry of Sediments and Sedimentary Rocks: Evolutionary Considerations to Mineral Deposit-Forming Environments*. Geological Association of Canada, *GEOtext* 4, pp 105–120
- DEER WA, HOWIE RA, ZUSSMAN J (1997) *Rock-forming Minerals*, vol. 1A, Orthosilicates. The Geological Society, London, pp 1–764
- DILL HG, TECHMER A, WEBER B, FÜSSL M (2008) Mineralogical and chemical distribution patterns of placers and ferricretes in Quaternary sediments in SE Germany: the impact of nature and man on the unroofing of pegmatites. *J Geochem Explor* 96: 1–24
- ERSHOVA V, HOLBROOK J, KHUDDOLEY A, PROKOPIEV A (2012) Priverkhoyansk foreland basin (eastern Siberia): interaction between fold-thrust belt tectonics and sedimentary supply. *Geol Soc Am Abst with Programs* 44: 175
- ERSHOVA VB, PROKOPIEV AV, KHUDDOLEY AK, SHNEIDER GV, ANDERSEN T, KULLERUD K, MAKAR'EV AA, MASLOV AV, KOLCHANOV DA (2015) Results of U–Pb (LA–ICPMS) dating of detrital zircons from metaterrigenous rocks of the basement of the North Kara Basin. *Dokl Earth Sci* 464: 997–1000
- ERSHOVA VB, KHUDDOLEY AK, PROKOPIEV AV, TUCHKOVA MI, FEDOROV PV, KAZAKOVA GG, SHISHLOV SB, O'SULLIVAN P (2016) Trans-Siberian Permian rivers: a key to understanding Arctic sedimentary provenance. *Tectonophysics*, 691: 220–233
- ERSHOVA VB, PROKOPIEV AV, KHUDDOLEY AK, PROSKURNIN VF, ANDERSEN T, KULLERUD K, STEPUNINA MA, KOLCHANOV DA (2017) New U–Pb isotopic data for detrital zircons from metasedimentary sequences of northwestern Taimyr. *Dokl Earth Sci* 474: 613–616
- FEDO CM, SIRCOMBE K, RAINBIRD R (2003) Detrital zircon analysis of the sedimentary record. In: HANCHAR MJ, HOSKIN PWO (eds) *Zircon. Reviews in Mineralogy and Geochemistry* 53: 277–303
- GEHRELS G (2012) Detrital zircon U–Pb geochronology: current methods and new opportunities. In: BUSBY C, AZOR A (eds) *Tectonics of Sedimentary Basins: Recent Advances*, Chapter 2. Blackwell Publishing Ltd., Hoboken, pp 47–62

- GEHRELS G (2014) Detrital zircon U–Pb geochronology applied to tectonics. *Ann Rev Earth Planet Sci* 42: 127–149
- GRÜTTER HS, GURNEY JJ, MENZIES AH, WINTER F (2004) An updated classification scheme for mantle-derived garnets, for use by diamond explorers. *Lithos* 77: 841–857
- HALLSWORTH CR, CHISHOLM JI (2008) Provenance of Late Carboniferous sandstones in the Pennine Basin (UK) from combined heavy mineral, garnet geochemistry and palaeocurrent studies. *Sedim Geol* 203: 196–212
- HENRY DJ, GUIDOTTI CV (1985) Tourmaline as a petrogenetic indicator mineral: an example from the staurolite-grade metapelites of NW Maine. *Amer Miner* 70: 1–15
- HENRY DJ, NOVÁK M, HAWTHORNE FC, ERTL A, DUTROW B, UHER P, PEZZOTTA F (2011) Nomenclature of the tourmaline-super group minerals. *Amer Miner* 96: 895–913
- IVANOV AV, HE H, YAN L, RYABOV VV, SHEVKO AY, PALESSKII SV, NIKOLAEVA IV (2013) Siberian Traps large igneous province: evidence for two flood basalt pulses around the Permo–Triassic boundary and in the Middle Triassic, and contemporaneous granitic magmatism. *Earth Sci Rev* 122: 58–76
- KAPLAN ME (1976) Lithology of Mesozoic Marine Sediments in Northern East Siberia. Nedra, Leningrad, pp 1–231 (in Russian)
- KHUDOLEY AK, PROKOPIEV AV (2007) Defining the eastern boundary of the North Asian Craton from structural and subsidence history studies of the Verkhojansk fold-and-thrust belt. In: SEARS JW, HARMS TA, EVENCHICK CA (eds) *Whence the Mountains? Inquiries into the Evolution of Orogenic Systems: A Volume in Honor of Raymond A. Price*. Geological Society of America, Special Papers 433: 391–410
- KHUDOLEY AK, KROPACHEV AP, TKACHENKO VI, RUBLEV AG, SERGEEV SA, MATUKOV DI, LYAHNITSKAYA OYU (2007) Meso- to Neoproterozoic evolution of the Siberian Craton and adjacent microcontinents: an overview with constraints for Laurentian connection. In: LINK PK, REED SL (eds) *Proterozoic Geology of Western North America and Siberia*. SEPM Special Publications 86: 209–226
- KHUDOLEY A, CHAMBERLAIN K, ERSHOVA V, SEARS J, PROKOPIEV A, MACLEAN J, KAZAKOVA G, MALYSHEV S, MOLCHANOV A, KULLERUD K, TORO J, MILLER E, VESELOVSKIY R, LI A, CHIPLEY D (2015) Proterozoic supercontinental restorations: constraints from provenance studies of Mesoproterozoic to Cambrian clastic rocks, eastern Siberian Craton. *Precambr Res* 259: 78–94
- KOWAL-LINKA M, STAWIKOWSKI W (2013) Garnet and tourmaline as provenance indicators of terrigenous material in epicontinental carbonates (Middle Triassic, S Poland). *Sedim Geol* 291: 27–47
- KRIPPNER A, MEINHOLD G, MORTON AC, VON EYNATTEN H (2014) Evaluation of garnet discrimination diagrams using geochemical data of garnets derived from various host rocks. *Sedim Geol* 306: 36–52
- KURAPOV MYU, ERSHOVA VB, MAKARIEV AA, MAKARIEVA EV, KHUDOLEY AK, LUCHITSKAYA MV, PROKOPIEV AV (2018) Carboniferous granitoid magmatism of Northern Taimyr: results of isotopic-geochemical study and geodynamic interpretation. *Geotectonics* 52: 229–235
- LORENZ H, GEE DG, SIMONETTI A (2008) Detrital zircon ages and provenance of the Late Neoproterozoic and Palaeozoic successions on Severnaya Zemlya, Kara Shelf: a tie to Baltica. *Norw J Geol* 88: 235–258
- LUDWIG KR (2012) *Isoplot 3.75, A Geochronological Toolkit for Microsoft Excel*: Berkeley Geochronology Center Special Publications No. 5, University of California at Berkeley, pp 1–75
- MAKARIEV AA (ed) (2013) *Geological Map of Russian Federation, scale 1:1000000, sheet T-45-48 (Cape Chelyuskin)*. Explanatory notes. VSEGEI, St. Petersburg, pp 1–472 (in Russian)
- MALICH NS (ed) (1999) *Geological Map of Siberian Platform and Adjoining Areas. Scale 1:1 500 000 (9 sheets)*. VSEGEI Press, St. Petersburg (in Russian)
- MALYSHEV SV, KHUDOLEY AK, PROKOPIEV AV, ERSHOVA VB, KAZAKOVA GG, TERYTYEVA LB (2016) Source rocks of Carboniferous–Lower Cretaceous terrigenous sediments of the northeastern Siberian Platform: results of Sm–Nd isotope–geochemical studies. *Russ Geol Geophys* 57: 421–433
- MANGE MA, MORTON AC (2007) Geochemistry of heavy minerals. *Devel Sedim* 58: 345–391
- MÉRES Š (2008) Garnets – important information resource about source area and parental rocks of the siliciclastic sedimentary rocks. In: JURKOVIČ Ľ (ed) *Conference “Cambelove dni 2008”*: Abstract Book. Comenius University, Bratislava, pp 37–43
- MORTON AC (1985) Heavy Minerals in provenance studies. In: ZUFFA GG (eds) *Provenance of Arenites*. NATO ASI Series (Series C: Mathematical and Physical Sciences) 148: Springer, Dordrecht, pp 249–277
- MORTON AC (1991) Geochemical studies of heavy minerals and their application to provenance research. In: MORTON AC, TODD SP, HAUGHTON PDW (eds) *Developments in Sedimentary Provenance Studies*. Geological Society of London Special Publications 57: 31–45
- PARFENOV LM, PROKOPIEV AV, GAIDUK VV (1995) Cretaceous frontal thrusts of the Verkhojansk fold belt, eastern Siberia. *Tectonics*, 14, 342–358
- PEASE V, SCOTT R (2009) Crustal affinities in the Arctic Uralides, northern Russia: significance of detrital zircon ages from Neoproterozoic and Palaeozoic sediments in Novaya Zemlya and Taimyr. *J Geol Soc, London* 166: 517–527
- POGREBITSKY YUE (ed) (1998) *State Geological Map of Russian Federation. Scale 1:1000000. Sheet S-47-49 (Lake Taimyr)*. VSEGEI, St. Petersburg (in Russian)
- POGREBITSKIY YUE, SHANURENKO NK (1998) *State Geological Map of the Russian Federation. Scale 1:1 000 000*.

- Sheet S-47-49 (Lake Taimyr). Explanatory Note. VSEGEI, St. Petersburg, pp 1–231 (in Russian)
- PROKOPIEV AV, PARFENOV LM, TOMSHIN MD, KOLODEZNIKOV II (2001) The cover of the Siberian Platform and adjacent fold–thrust belts. In: PARFENOV LM, KUZMIN MI (eds) *Tectonics, Geodynamics, and Metallogeny of the Sakha Republic (Yakutia)*. MAIK Nauka/Interperiodica, Moscow, pp 113–155 (in Russian)
- PUCHKOV VN (2009) The evolution of the Uralian Orogen. In: MURPHY JB, KEPPIE JD, HYNES AJ (eds) *Ancient Orogens and Modern Analogues*. Geological Society of London Special Publications 327: 161–195
- SMELOV AP, TIMOFEEV VF (2007) The age of the North Asian cratonic basement: an overview. *Gondwana Res* 12: 279–288
- SUGGATE SM, HALL R (2014) Using detrital garnet compositions to determine provenance: a new compositional database and procedure. In: SCOTT RA, SMYTH HR, MORTON AC, RICHARDSON N (eds) *Sediment Provenance Studies in Hydrocarbon Exploration and Production*. Geological Society of London Special Publications 386: 373–393
- TERAOKA Y, SUZUKI M, HAYASHI T, KAWAKAMI K (1997) Detrital garnets from Paleozoic and Mesozoic sandstones in the Onogawa area, East Kyushu, Southwest Japan. *Bull Fac Sch Educ, Hiroshima University, Part II* 19: 87–101 (in Japanese with English abstract)
- TERAOKA Y, SUZUKI M, KAWAKAMI K (1998) Provenance of Cretaceous and Paleogene sediments in the Median Zone of Southwest Japan. *Bull Geol Soc Jap* 49: 395–411 (in Japanese with English abstract)
- VAN HINSBERG VJ, HENRY DJ, DUTROW BL (2011) Tourmaline as a petrologic forensic mineral: a unique recorder of its geologic past. *Elements* 7: 327–332
- VĎAČNÝ M, BAČÍK P (2015) Provenance of the Permian Malužiná Formation sandstones (Malé Karpaty Mountains, Western Carpathians): evidence of garnet and tourmaline mineral chemistry. *Geol Carpath* 66: 83–97
- VERNIKOVSKY VA (1996) Geodynamic Evolution of Taimyr Fold Area. SB RAS, Novosibirsk, pp 1–202 (in Russian)
- VERNIKOVSKY VA, PEASE VL, VERNIKOVSKAYA AE, ROMANOV AP, GEE DG, TRAVIN AV (2003) First report of early Triassic A-type granite and syenite intrusions from Taimyr: product of the northern Eurasian superplume. *Lithos* 66: 23–36
- VYSSOTSKI AV, VYSSOTSKI VN, NEZH DANOV AA (2006) Evolution of the West Siberian Basin. *Mar Petrol Geol* 23: 93–126
- WRIGHT WI (1938) The composition and occurrence of garnets. *Amer Miner* 23: 436–449
- ZHANG X, OMM A J, PEASE V, SCOTT R (2013) Provenance of late Paleozoic–Mesozoic sandstones, Taimyr Peninsula, the Arctic. *Geosciences* 3: 502–527
- ZHANG X, PEASE V, OMM A V, BENEDICTUS A (2015) Provenance of Late Carboniferous to Jurassic sandstones for southern Taimyr, Arctic Russia: a comparison of heavy mineral analysis by optical and QEMSCAN methods. *Sedim Geol* 329: 166–176
- ZONENSHAIN LP, KUZMIN MI, NATAPOV LM, PAGE BM (1990) *Geology of the USSR: a plate tectonic synthesis*. American Geophysical Union. *Geodynamics Series* 21: pp 1–242